

Supplementary Materials for

Effect of Processing and End Groups on the Crystal Structure of Polypeptoids Studied by Cryogenic Electron Microscopy on Atomic Length Scales

Xi Jiang^{1&}, *Sunting Xuan*^{2&}, *Joyjit Kundu*^{2#}, *David Prendergast*², *Ronald N. Zuckermann*^{2*},
Nitash P. Balsara^{1,3*}

¹ Materials Sciences Division, Lawrence Berkeley National Laboratory, Berkeley, CA 94720, United States.

² Molecular Foundry, Lawrence Berkeley National Laboratory, Berkeley, CA 94720, United States.

³ College of Chemistry, University of California, Berkeley, CA 94720, United States.

& Authors contributed equally.

[#] Present address: Department of Chemistry, Duke University, Durham, North Carolina 27708 United States

* *Corresponding authors: rnzuckermann@lbl.gov; nbalsara@berkeley.edu.*

Submission to Soft Matter

List of supplementary materials:

Figure S1. LC-MS trace of pNdc₉-pNte₉ solution

Figure S2. LC-MS trace of Cl-pNdc₉-pNte₉ solution

Figure S3. LC-MS trace of I-pNdc₉-pNte₉ solution

Figure S4. TEM micrograph of pNdc₉-pNte₉ nanosheets obtained by very slow evaporation.

Table S1. Parameters of analyzed cryo-EM micrographs

Figure S5. FFTs of Motifs in pNdc₉-pNte₉ nanosheets obtained by difference processes.

Figure S6. Structure of the self-assembled Cl-pNdc₉-pNte₉ and I-pNdc₉-pNte₉ nanosheets prepared by very slow evaporation.

Figure S7. Motifs in Cl-pNdc₉-pNte₉ and I-pNdc₉-pNte₉ nanosheets prepared by very slow evaporation.

Figure S8. FFTs of Motifs in Cl-pNdc₉-pNte₉ and I-pNdc₉-pNte₉ nanosheets in Figure S7.

Figure S9. Distribution maps of motifs in the nanosheets

Figure S10. Rotation average 1-D plots of FFTs in Figure 3 and the indexed Miller indices.

Figure S11. AFM height image of nanosheets prepared by fast evaporation.

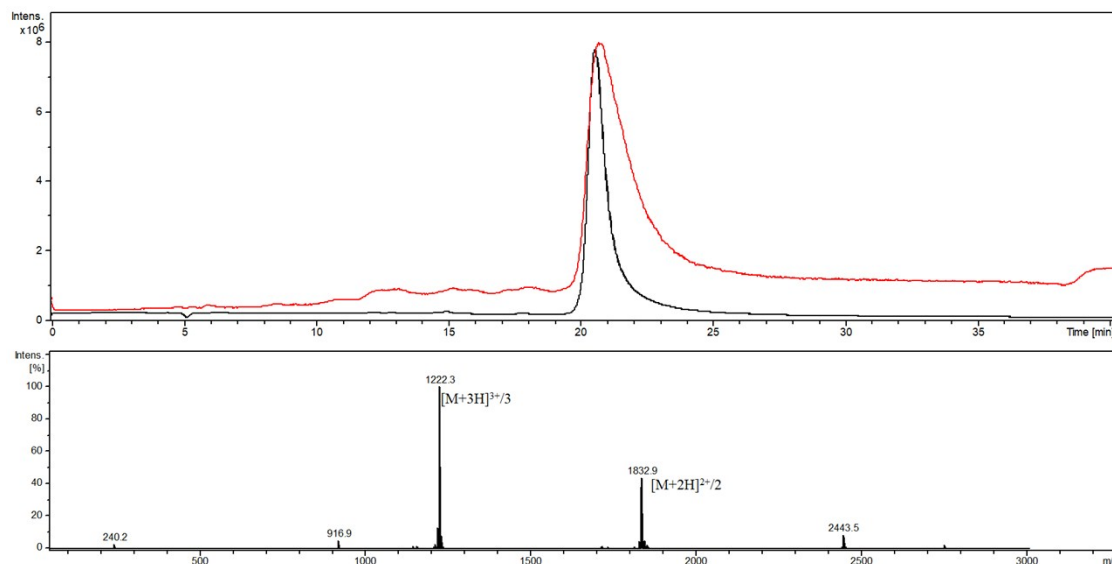


Figure S1. LC-MS trace of Ndc₉-Nte₉ sheet solution. with gradient of 70-95% solvent B in 20 min (B is 10% isopropanol in acetonitrile and A is 10% isopropanol in water). Black plot in top panel represents LC trace; red plot in top panel represents total ion chromatogram and bottom panel shows mass spectrum. Note: the sheet solution was lyophilized and re-dissolved in a mixture of acetonitrile/isopropanol/water for LC-MS analysis.

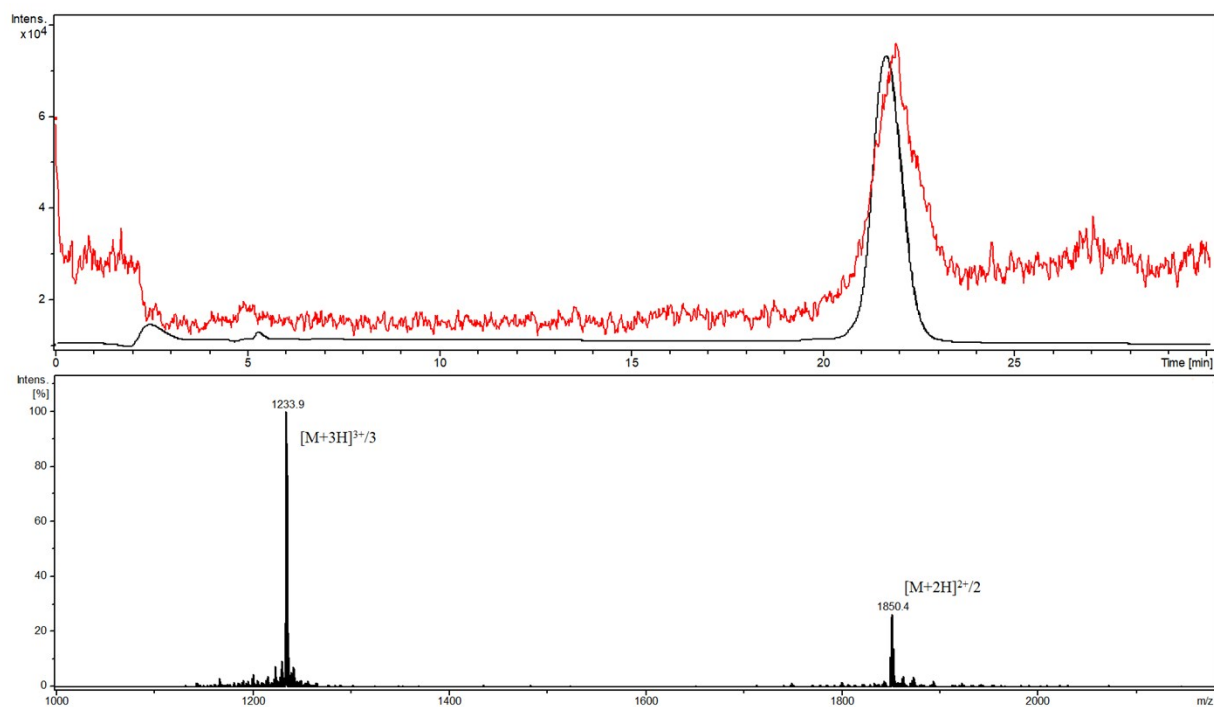


Figure S2. LC-MS trace of CI-Ndc₉-Nte, sheet solution. with gradient of 70-95% solvent B in 20 min (B is 10% isopropanol in acetonitrile and A is 10% isopropanol in water). Black plot in top panel represents LC trace; red plot in top panel represents total ion chromatogram and bottom panel shows mass spectrum. Note: the sheet solution was lyophilized and re-dissolved in a mixture of acetonitrile/isopropanol/water for LC-MS analysis.

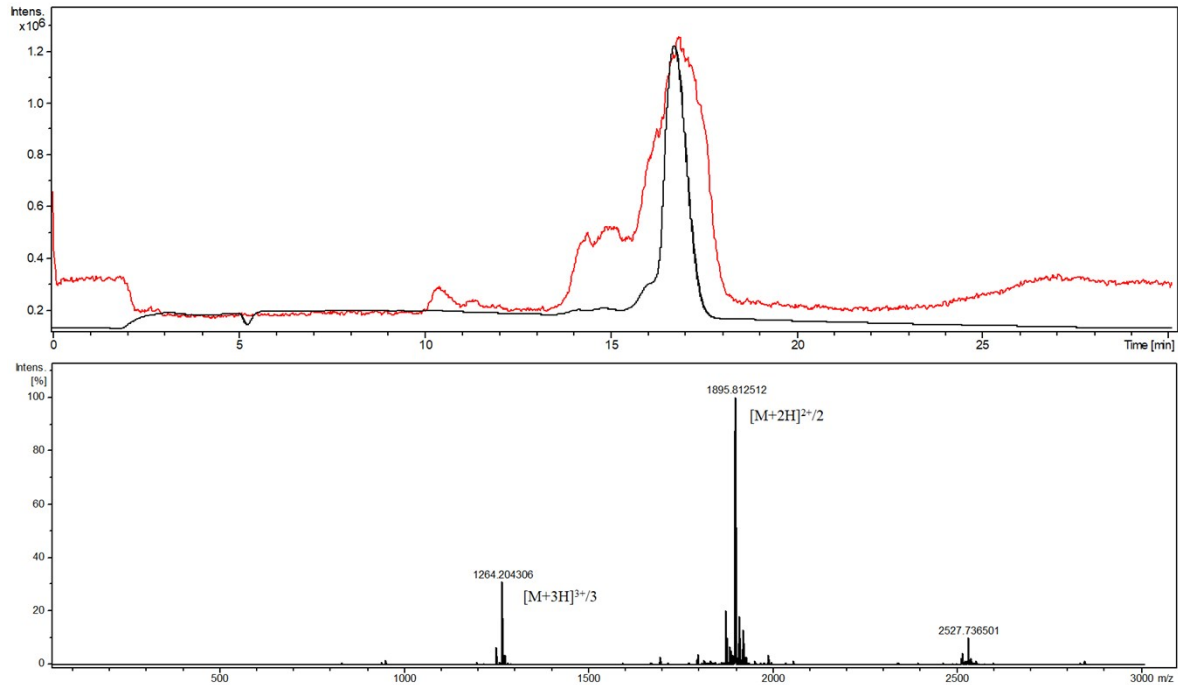


Figure S3. LC-MS trace of I-Ndc₉-Nte₉ sheet solution. with gradient of 75-95% solvent B in 20 min (B is 10% isopropanol in acetonitrile and A is 10% isopropanol in water). Black plot in top panel represents LC trace; red plot in top panel represents total ion chromatogram and bottom panel shows mass spectrum. Note: the sheet solution was lyophilized and re-dissolved in a mixture of acetonitrile/isopropanol/water for LC-MS analysis.

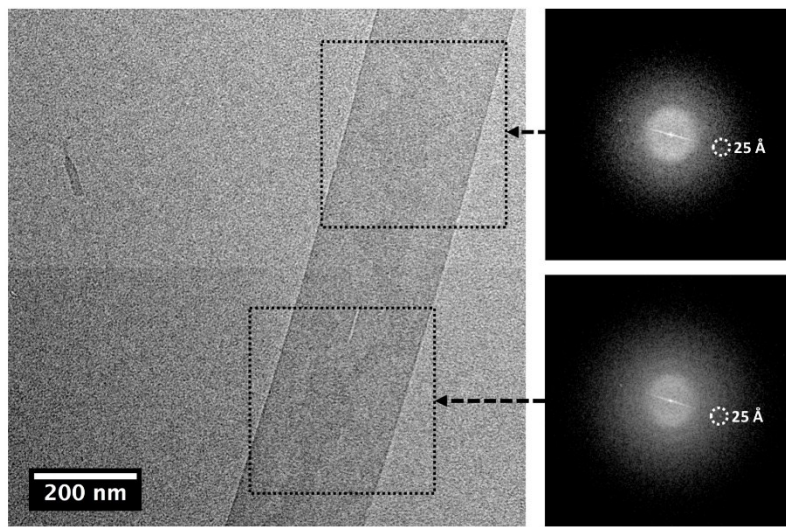


Figure S4. TEM micrograph of pNdc₉-pNte₉ nanosheets obtained by very slow evaporation. The Fourier transforms obtained at different positions along a ribbon like nanosheet show identical featured reflections at 25 Å which suggest the presence of long-range order in polypeptoid crystalline nanosheets

Table S1. Parameters of analyzed cryo-EM micrographs

Nanosheets	Number of micrographs	Defocus range ^a	Number of boxes extracted from the micrographs	Highest resolution of Thon rings in the FFTs of micrographs ^a	Highest resolution of reflections in the FFTs of averaged images
pNdc ₉ -pNte ₉ (fast)	12	6595-11143 Å	166117	2.7-2.9 Å	2.1 Å
pNdc ₉ -pNte ₉ (medium)	4	5451-7765 Å	70902	1.9-3.0 Å	2.4 Å
pNdc ₉ -pNte ₉ (slow)	10	2773-4978 Å	262826	1.9-2.5 Å	2.1 Å
Cl-pNdc ₉ -pNte ₉ (slow)	13	2825-5139 Å	346113	1.9-2.4 Å	2.1 Å
I-pNdc ₉ -pNte ₉ (slow)	4	2484-2960 Å	56860	1.9-2.6 Å	2.1 Å

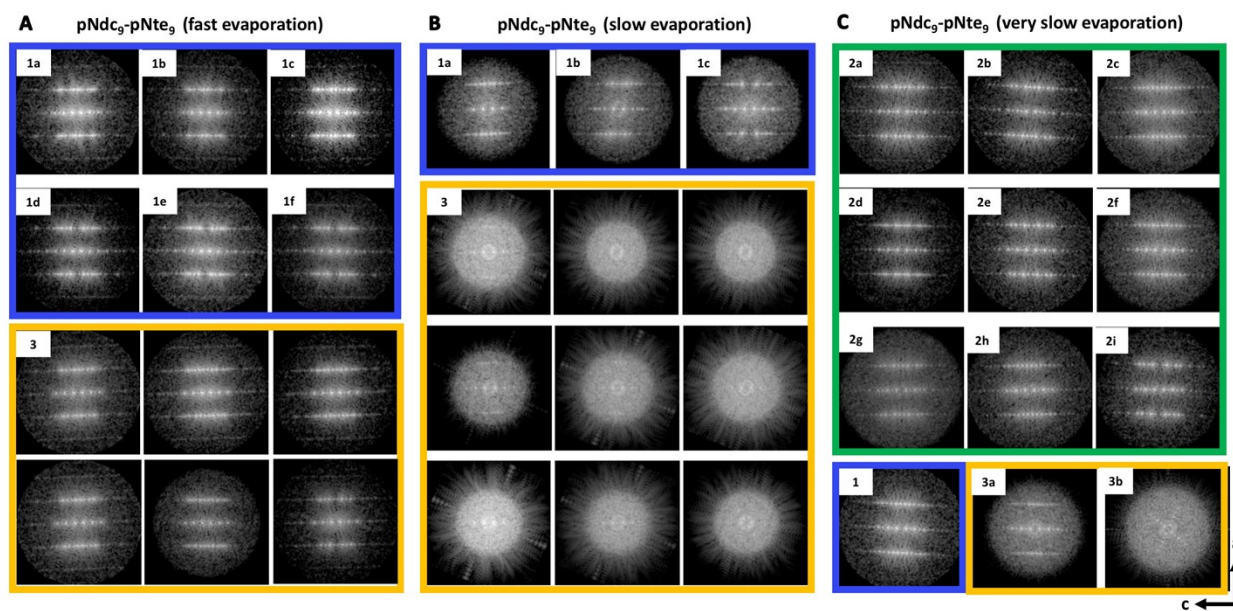


Figure S5. FFTs of Motifs in $pNdc_9$ - $pNte_9$ nanosheets obtained by difference processes. As described in Figure 4, boxes were sorted and averaged assuming the presence of 12 classes. These classes naturally fall into two distinct groups that contain ordered motifs: anti-parallel V-shaped motifs (group 1 identified by a blue outline), parallel V-shaped motifs (group 2 identified by a green outline). Classes that were inconsistent with the molecule shown in Figure 1C are collectively referred to as disordered (group 3 identified by a yellow outline). FFTs of motifs in the $pNdc_9$ - $pNte_9$ nanosheets obtained by **A**: fast evaporation, **B**: slow evaporation, **C**: very slow evaporation. The a and c dimensions demonstrate the spacings as shown in the atomic model in Figure 1C. Bright areas in all images represent the electron dense regions. The a and c dimensions demonstrate the spacings as shown in the atomic model in Figure 1B and Figure 5.

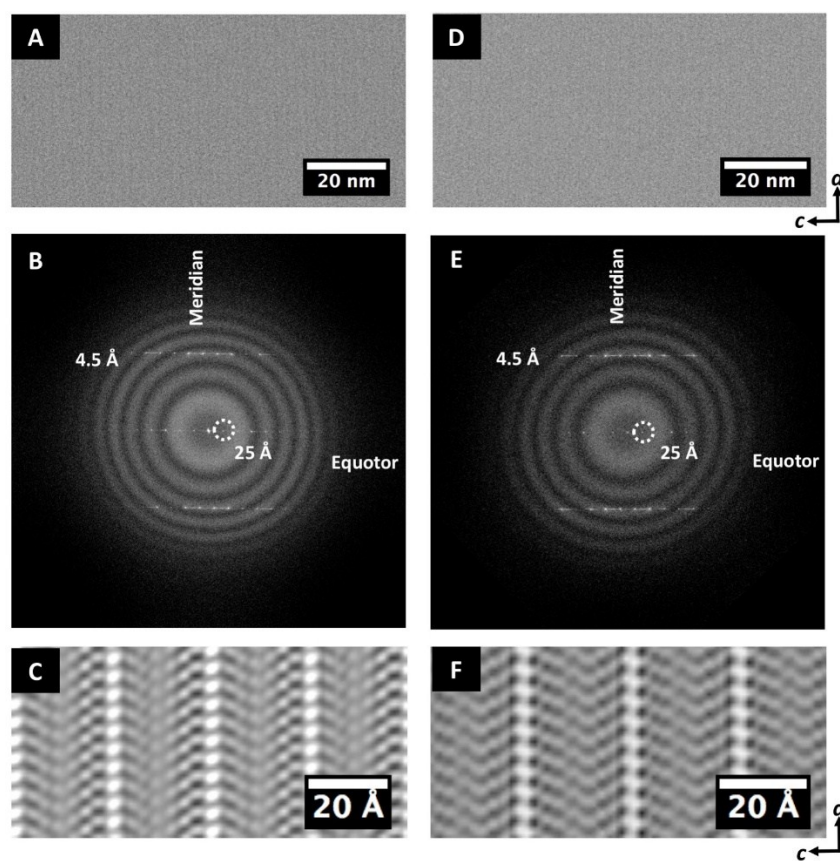


Figure S6. Structure of the self-assembled Cl-pNdc₉-pNte₉ and I-pNdc₉-pNte₉ nanosheets prepared by very slow evaporation. **A.** A section of a low-dose cryo-EM micrograph of vitrified hydrated Cl-pNdc₉-pNte₉ nanosheets. **B.** The FFT of the low-dose cryo-EM micrograph in A showing reflections and Thon rings due to the thin carbon support. The dashed circle indicates the reflection corresponding to 25 Å which is the spacing between adjacent rows of pNdc backbones. The reflections at 4.5 Å indicate the spacing between two pNdc backbones. **C.** A section of Fourier filtered image of FFT in B. Reflections in B are filtered by applying a mask with 1 pixel diameter at each reflection. **D.** A section of a low-dose cryo-EM micrograph of vitrified hydrated I-pNdc₉-pNte₉ nanosheets. **E.** The FFT of the low-dose cryo-EM micrograph in D showing reflections and Thon rings due to the thin carbon support. The dashed circle indicates the reflection corresponding to 25 Å which is the spacing between adjacent rows of pNdc backbones. The reflections at 4.5 Å

indicate the spacing between two pNdc backbones. **F.** A section of Fourier filtered image of FFT in E. Reflections in E are filtered by applying a mask with 1 pixel diameter at each reflection. Bright areas in all images represent the electron dense regions. The high symmetry images in C, F, and J are artifacts due to averaging over distinct motifs.

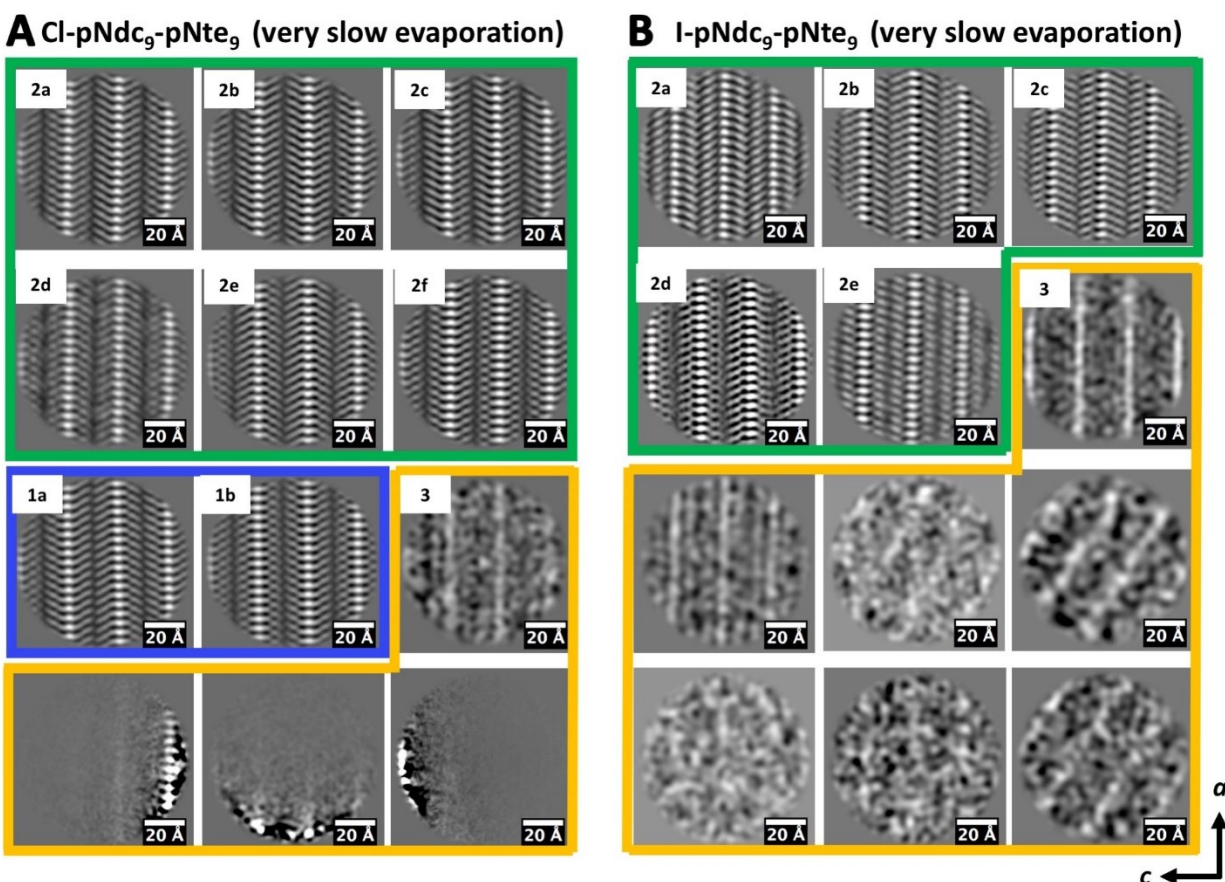


Figure S7. Motifs in Cl-pNdc₉-pNte₉ and I-pNdc₉-pNte₉ nanosheets prepared by very slow evaporation. Boxes were sorted and averaged assuming the presence of 12 classes. These classes naturally fall into two distinct groups that contain ordered motifs: anti-parallel V-shaped motifs (group 1 identified by a blue outline), parallel V-shaped motifs (group 2 identified by a green outline). Classes that were inconsistent with the molecule shown in Figure 1C are collectively referred to as disordered (group 3 identified by a yellow outline). **A.** Motifs of Cl-pNdc₉-pNte₉ nanosheets, **B:** Motifs of I-pNdc₉-pNte₉ nanosheets. The *a* and *c* dimensions demonstrate the spacings as shown in the atomic model in Figure 1C. Bright areas in all images represent the electron dense regions.

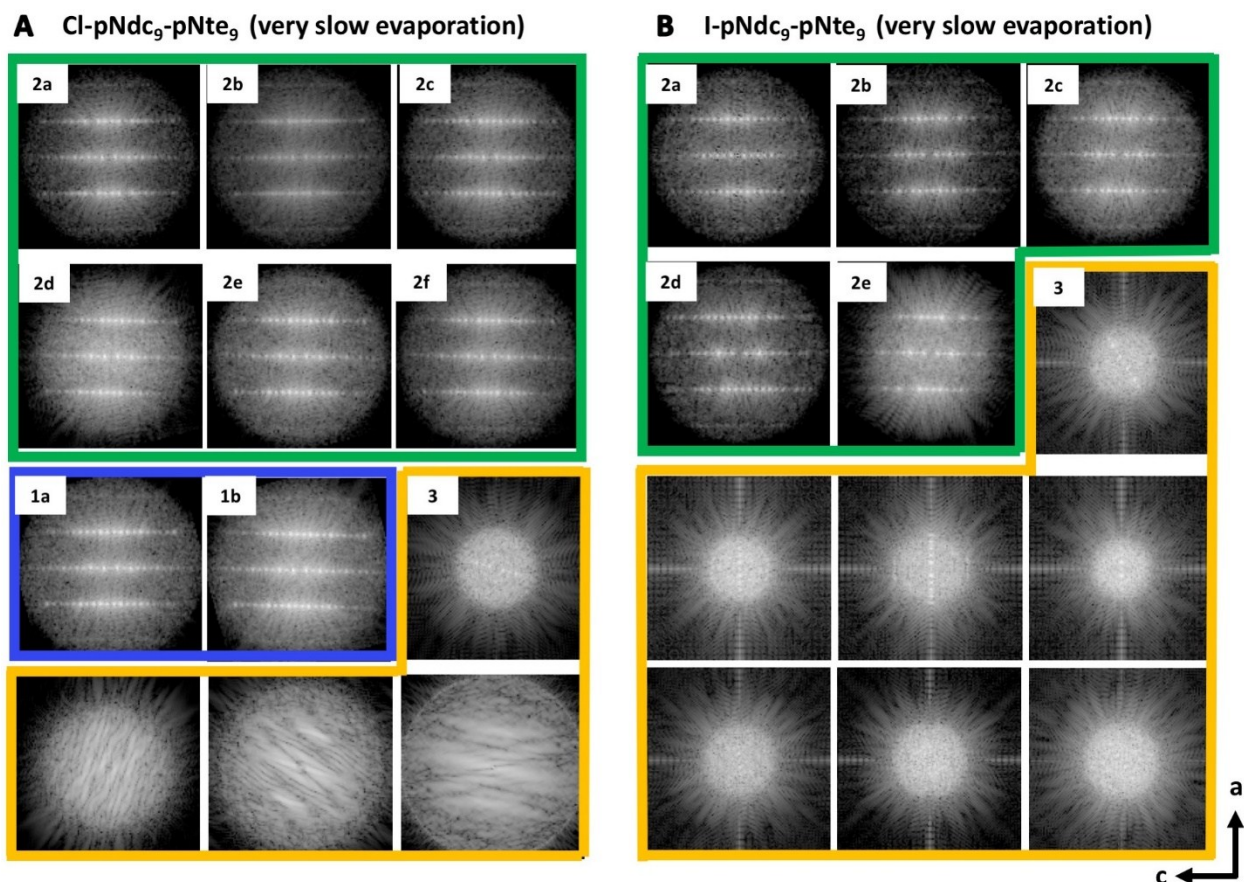


Figure S8. FFTs of Motifs in Cl-pNdc₉-pNte₉ and I-pNdc₉-pNte₉ nanosheets shown in Figure S7. As described in Figure S4, boxes were sorted and averaged assuming the presence of 12 classes. These classes naturally fall into two distinct groups that contain ordered motifs: anti-parallel V-shaped motifs (group 1 identified by a blue outline), parallel V-shaped motifs (group 2 identified by a green outline). Classes that were inconsistent with the molecule shown in Figure 1C are collectively referred to as disordered (group 3 identified by a yellow outline). **A.** The FFTs of anti-parallel V-shaped motifs, parallel V-shaped motifs and disordered motifs in Cl-pNdc₉-pNte₉ nanosheets. **B.** The FFTs of parallel V shape motifs and unidentified motifs in I-pNdc₉-pNte₉ (slow) nanosheets. The *a* and *c* dimensions demonstrate the spacings as same as these shown in the atomic model in Figure 1B.

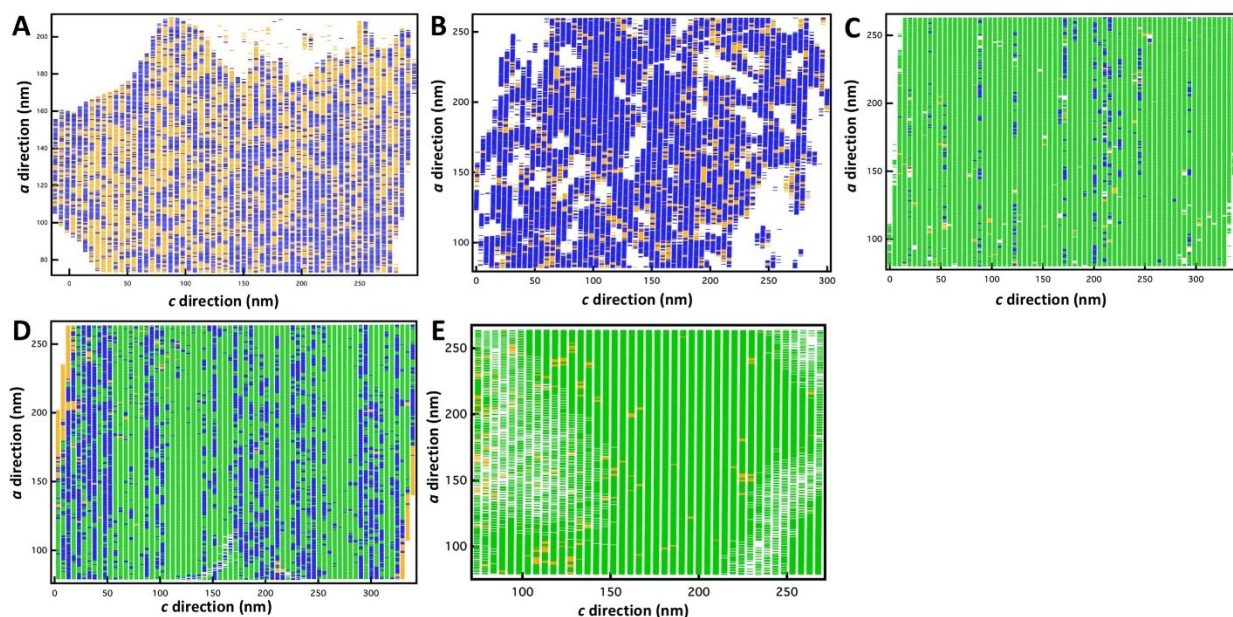


Figure S9. Distribution maps of motifs in the polypeptoid nanosheets Each individual rectangle in the maps represents a unit cell. Anti-parallel V-shaped motifs are shown as blue boxes. Parallel V-shaped motifs are shown as green boxes. Disordered motifs are shown as yellow boxes. **A:** pNdc₉-pNte₉ nanosheet obtained by fast evaporation, **B:** pNdc₉-pNte₉ nanosheet obtained by slow evaporation, **C:** pNdc₉-pNte₉ nanosheet obtained by very slow evaporation. **D:** Cl-pNdc₉-pNte₉ nanosheet obtained by very slow evaporation, **E:** I-pNdc₉-pNte₉ nanosheet obtained by very slow evaporation. White areas within the maps represent the regions that were not analyzed.

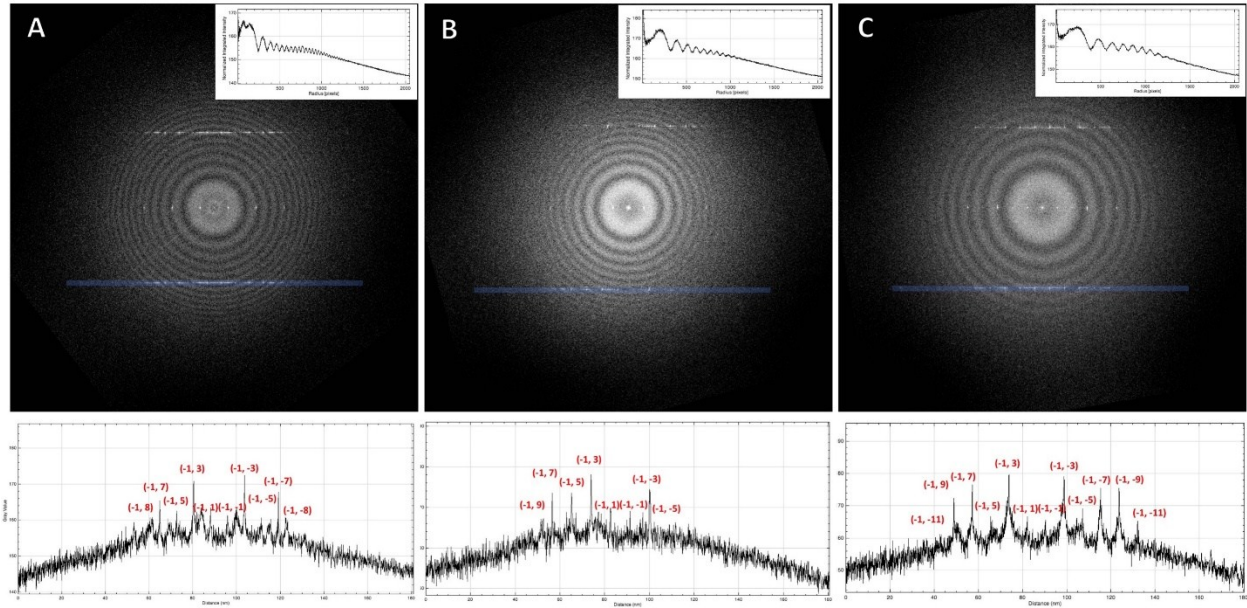


Figure S10. Rotation average 1-D plots of FFTs in Figure 3 and the indexed Miller indices.

Insets represent the 1-D rotationally averaged FFTs and the bottom panel show the line profiles as indicated by blue lines in FFTs. Miller indices are shown in red **A**, fast evaporation, **B**: slow evaporation, **C**: very slow evaporation.

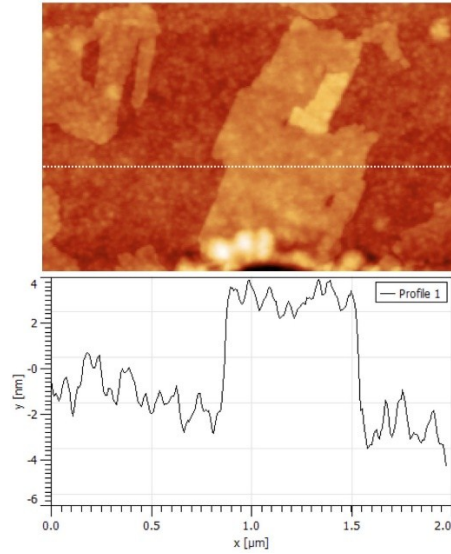


Figure S11. AFM height image of nanosheets prepared by fast evaporation. Top panel shows the AFM height image. White dotted line represents the position of measured thickness profile of a monolayer nanosheet (shown in bottom panel)